РОЗДІЛ 5. АВТОМАТИЗАЦІЯ ЕЛЕКТРОМЕХАНІЧНИХ СИСТЕМ ТА ЕЛЕКТРОПРИВОД

FEEDBACK LINEARIZING CONTROL ALGORITHMS FOR SALIENT POLE SYNCHRONOUS MOTORS CONSIDERING SATURATION AND CROSS-COUPLING

Rodkin D., PhD student, Zinchenko O., student, Peresada S., prof., Pyzhov V., associate prof.
Igor Sikorsky Kyiv Polytechnic Institute, department of automation of electromechanical systems and electric drives

Introduction. Salient pole synchronous motors found their application in many fields, due to better flux weakening capability and stability [1]. Representatives of this type of motors are interior permanent magnets synchronous motors (IPMSMs) which is characterized by high torque and power density and synchronous reluctance motors (SynRMs). Simple and rugged construction, higher efficiency compared to an induction motor due to rotor windings absence are main features of the SynRMs [2]. In many aspects SynRMs are similar to IPMSMs except absence of permanent magnets in the rotor [3].

Vector control is usually used to control IPMSMs and SynRMs. Saturation and cross-coupling effects for these motors are more distinct due to saliency. If conventional vector control algorithm is applied to such motors, control performance may deteriorate due to magnetic saturation [4].

Different approaches were proposed to take into account saturation effects and eliminate its impact on control algorithms. In [4] self and cross-inductances are determined by magnetic flux fitting coefficients and used during decoupling control algorithm synthesis. Other approach proposed MTPA (Maximum Torque per Ampere) tracking method, which is insensitive to inductances variation [5]. Improvement of torque estimation for IPMSM torque control was presented in [6] using high-frequency injection-based determination of cross-saturation inductances. In [7] magnetic system saturation is considered to improve flux-weakening references and voltage restrictions. High harmonic components of the inductances considering cross and self-saturation from flux Fourier analysis are presented to modify IPMSM model in [8]. Estimated self- and cross-inductances are used to generate compensation of back emf components in [9]. In [10] fitted flux maps boundaries are used for improving several control strategies.

Purpose. To validate necessity of usage of algorithms with saturation and cross-coupling consideration to achieve high precision operation.

Material of the research. General model considering saturation and cross – coupling for synchronous motors with saliency in matrix form is presented below [11]

$$\frac{d\omega}{dt} = \frac{3}{2}\frac{p_n}{J}\boldsymbol{\Psi}^T\mathbf{J}^T\mathbf{i} - \frac{\nu}{J}\omega - \frac{T_L}{J}, \quad (1)$$

$$\mathbf{L}\dot{\mathbf{i}} = -R\mathbf{i} - p_n\omega\mathbf{J}\boldsymbol{\Psi} + \mathbf{u}, \quad (2)$$

$$\dot{\boldsymbol{\Psi}} = \mathbf{L}\dot{\mathbf{i}}, \tag{3}$$

where ω - angular speed, p_n - number of pole pairs, J - total moment of inertia, ν - viscous friction, T_L - load torque, $\boldsymbol{\Psi} = \left[\Psi_d\left(i_d, i_q\right) \quad \Psi_q\left(i_d, i_q\right)\right]^T$ - fluxes along (d-q) axes, $\mathbf{i} = \left[i_d \quad i_q\right]^T$ - currents along (d-q) axes, $\mathbf{u} = \left[u_d \quad u_q\right]^T$ - voltages along (d-q) axes, R is resistance, $\mathbf{J} = \begin{bmatrix} 0 & -1 \\ 1 & 0 \end{bmatrix}$, $\mathbf{L} = \begin{bmatrix} L_{dd}\left(i_d, i_q\right) & L_{dq}\left(i_d, i_q\right) \\ L_{qd}\left(i_d, i_q\right) & L_{qq}\left(i_d, i_q\right) \end{bmatrix}$ are dynamic inductances that are calculated as follows

$$\begin{aligned} L_{dd}\left(i_d, i_q\right) &= \frac{\partial \Psi_d\left(i_d, i_q\right)}{\partial i_d}; L_{qq}\left(i_d, i_q\right) = \frac{\partial \Psi_q\left(i_d, i_q\right)}{\partial i_q}; \\ L_{dq}\left(i_d, i_q\right) &= \frac{\partial \Psi_d\left(i_d, i_q\right)}{\partial i_q}; L_{qd}\left(i_d, i_q\right) = \frac{\partial \Psi_q\left(i_d, i_q\right)}{\partial i_d}. \end{aligned} \tag{4}$$

With the purpose of achieving more readable and compact algorithm derivation, inductances and fluxes will be shown without $\left(i_d, i_q\right)$ in further section.

Formulation of the control problem. Following assumptions (A) are taken:

A.1. Stator currents, angular speed and angular position are measured values.

A.2. Parameters of the motor are known. Fluxes curves $\Psi_d\left(i_d, i_q\right)$, $\Psi_q\left(i_d, i_q\right)$ along (d-q) axes are smooth and known.

A.3. Torque T_L is unknown, limited, constant or those that is changing slowly.

A.4. The rotor speed reference ω^* is smooth and bounded function together with its first $\dot{\omega}^*$ and second $\ddot{\omega}^*$ time derivatives; d-axis current reference i_d^* is bounded together with its bounded derivative $\dot{i}_d^*$.

A.5. Both saturation and cross-coupling are considered in the control algorithm.

The control problem is to design a speed controller, which guarantees following control objectives (CO):

CO.1. Asymptotic speed ω and direct current component i_d tracking:

$$\lim_{t \to \infty}\left(\tilde{\omega}, \tilde{i}_d\right) = 0, \tag{5}$$

where $\tilde{\omega} = \omega - \omega^*$ - rotor speed error, $\tilde{i}_d = i_d - i_d^*$ - direct current component error.

CO.2. Asymptotic decoupling of speed control and direct current control subsystems.

CO.3. Linearization of speed control subsystem.

Design of the control algorithm with full compensation of cross-coupling and saturation. Current reference i_q^* is formed basing on (1):

$$\begin{aligned} i_q^* &= \frac{1}{\mu \Psi_d}\left(\mu \Psi_q i_d^* + \frac{\nu}{J}\omega^* + \dot{\omega}^* - k_\omega \tilde{\omega} + \hat{T}_L\right), \\ \dot{\hat{T}}_L &= -k_{\omega i}\tilde{\omega}, \end{aligned} \tag{6}$$

where $\mu = \frac{3}{2}\frac{p_n}{J}$.

Speed error dynamics from (1), (6) is

$$\begin{aligned} \dot{\tilde{\omega}} &= \frac{3}{2}\frac{1}{J}p_n\left(\Psi_d\left(i_d, i_q\right)\tilde{i}_q - \Psi_q\left(i_d, i_q\right)\tilde{i}_d\right) - \left(\frac{\nu}{J} + k_\omega\right)\tilde{\omega} - \tilde{T}_L, \\ \dot{\tilde{T}}_L &= k_{\omega i}\tilde{\omega}, \end{aligned} \tag{7}$$

where $\tilde{i}_q = i_q - i_q^*$ is q-axis current error.

Information about q-axis current reference derivative $\dot{i}_q^*$ is required for current controllers. For this purpose, derivative from (7) is taken. Considering relations (2), (3) and (7), $\dot{i}_q^*$ can be found from the following equation

$$\dot{i}_q^* = \dot{i}_{q1}^* - \dot{\tilde{i}}_q x_1 + \dot{\tilde{i}}_d x_2 + \dot{i}_{q2}^*, \tag{8}$$

where $x_1 = \frac{-L_{qq}i_d^* + L_{dq}i_q^*}{\Psi_d + L_{dq}i_q^* - L_{qq}i_d^*}, x_2 = \frac{-L_{dd}i_q^* + L_{qd}i_d^*}{\Psi_d + L_{dq}i_q^* - L_{qq}i_d^*}, \dot{i}_{q2}^* = \frac{k_\omega \tilde{T}_L}{\mu\left(\Psi_d + L_{dq}i_q^* - L_{qq}i_d^*\right)},$

$$\dot{i}_{q1}^* = \left[\frac{\nu}{J}\dot{\omega}^* + \ddot{\omega}^* - k_\omega\left(\mu\left(\Psi_d\tilde{i}_q - \Psi_q\tilde{i}_d\right) - \left(\frac{\nu}{J} + k_\omega\right)\tilde{\omega}\right) - k_{\omega i}\tilde{\omega} + \mu\dot{i}_d^*\left(\Psi_q + L_{qd}i_d^* - L_{dd}i_q^*\right)\right] \div$$

$$\div\left(\mu\left(\Psi_d + L_{dq}i_q^* - L_{qq}i_d^*\right)\right).$$

From (8) is clear that $\dot{\tilde{\mathbf{i}}} = \begin{bmatrix}\dot{\tilde{i}}_d & \dot{\tilde{i}}_q\end{bmatrix}^T$ is presented in the expression, so $\dot{i}_q^*$ cannot be calculated directly from (8). Therefore, it is proposed to substitute (8) into current dynamics (2). After some simplifications, current error dynamics has the following form

$$\mathbf{L}_1\dot{\tilde{\mathbf{i}}} = -R\mathbf{i} - \omega p_n \mathbf{J}\boldsymbol{\Psi} + \mathbf{u} - \mathbf{L}\dot{\mathbf{i}}_1^* - \mathbf{L}\dot{\mathbf{i}}_2^* \tag{9}$$

where $\mathbf{L}_1 = \begin{bmatrix} L_{dd} + L_{dq}x_2 & L_{dq}\left(1 - x_1\right) \\ L_{qd} + L_{qq}x_2 & L_{qq}\left(1 - x_1\right)\end{bmatrix}, \dot{\mathbf{i}}_1^* = \begin{bmatrix}\dot{i}_d^* \\ \dot{i}_{q1}^*\end{bmatrix}, \dot{\mathbf{i}}_2^* = \begin{bmatrix}0 \\ \dot{i}_{q2}^*\end{bmatrix}.$

Current regulators can be derived from (9) as

$$\begin{aligned} \mathbf{u} &= R\mathbf{i} + \omega p_n \mathbf{J}\boldsymbol{\Psi} + \mathbf{L}\dot{\mathbf{i}}_1^* + \mathbf{L}_1\left(-\mathbf{K}_i\tilde{\mathbf{i}} - \mathbf{x}\right) \\ \dot{\mathbf{x}} &= \mathbf{K}_{ii}\tilde{\mathbf{i}} \end{aligned} \tag{10}$$

where $\mathbf{K}_i = \begin{bmatrix} k_i & 0 \\ 0 & k_i\end{bmatrix}$, $\mathbf{K}_{ii} = \begin{bmatrix} k_{ii} & 0 \\ 0 & k_{ii}\end{bmatrix}$, $\mathbf{x} = \begin{bmatrix}x_d \\ x_q\end{bmatrix}$, $\left(k_i, k_{ii}\right) > 0$ are proportional and integral gains of the current controller.

Current error dynamics can be obtained after substitution of (10) into (9)

$$\dot{\tilde{\mathbf{i}}} = -\mathbf{K}_i\tilde{\mathbf{i}} - \mathbf{x} - \mathbf{L}_1^{-1}\mathbf{L}\dot{\mathbf{i}}_2^* \tag{11}$$

Dynamics (11) in algebraic form is

$$\begin{aligned} \dot{\tilde{i}}_d &= -k_i\tilde{i}_d + x_d, \\ \dot{x}_d &= -k_{ii}\tilde{i}_d, \end{aligned} \tag{12}$$

$$\dot{\tilde{i}}_q = -k_i \tilde{i}_q + x_q - \frac{k_\omega \tilde{T}_L}{\mu \Psi_d},$$
$$\dot{x}_q = -k_{ii} \tilde{i}_q, \tag{13}$$

Direct axis current error dynamics (12) is linear and exponentially stable $\forall (k_i, k_{ii}) > 0$. Therefore condition

$$\lim_{t \to \infty} (\tilde{i}_d, x_d) = 0 \tag{14}$$

is fulfilled. Also dynamics (12) is completely decoupled from speed control subsystem dynamics (7), (13).

Speed control subsystem (7), (13) is asymptotically linear considering (14). Worth mentioning that Ψ_d in (6) and (13) has to be nonzero. This condition is always met for IPMSMs. In case of SynRMs it is required to modify speed controller to avoid division on zero. Equations (7) represent speed control loop, equations (13) – current control loop. Stability of the speed control subsystem can always be achieved with suitable tuning of the controller gains $(k_\omega, k_{\omega i}) > 0$ and $(k_i, k_{ii}) > 0$. According to the theory of the cascaded systems, speed control loop has to be at least two times slower that current control loop. With proposed coefficients tuning objectives CO.1. – CO.3. are satisfied.

Control algorithm without cross-coupling compensation. Flux curves are simplified comparing to the algorithm with full compensation so that $\Psi_d(i_d)$ $\Psi_q(i_q)$ are dependent on self-currents only. As a result, inductances (4) are determined as

$$L_{dd}(i_d) = \frac{\partial \Psi_d(i_d)}{\partial i_d}; L_{qq}(i_q) = \frac{\partial \Psi_q(i_q)}{\partial i_q}; L_{dq} = 0; L_{qd} = 0. \tag{15}$$

Speed controller (6) remains the same except for the fact that fluxes depend only on self-currents. Current controller (10) is modified considering abovementioned simplifications.

$$\mathbf{u} = R\mathbf{i} + \omega p_n \mathbf{J}\boldsymbol{\Psi}' + \mathbf{L}'\dot{\mathbf{i}}_1^* + \mathbf{L}_1'(-\mathbf{K}_i\tilde{\mathbf{i}} - \mathbf{x}),$$
$$\dot{\mathbf{x}} = \mathbf{K}_{ii}\tilde{\mathbf{i}}, \tag{16}$$

where $\boldsymbol{\Psi}' = \begin{bmatrix} \Psi_d(i_d) \\ \Psi_q(i_q) \end{bmatrix}$, $\mathbf{L}' = \begin{bmatrix} L_{dd}(i_d) & 0 \\ 0 & L_{qq}(i_q) \end{bmatrix}$, $\mathbf{L}_1' = \begin{bmatrix} L_{dd}(i_d) & 0 \\ L_{qq}(i_q)x'_2 & (1 - x'_1)L_{qq}(i_q) \end{bmatrix}$,

$x'_1 = \frac{-L_{qq}(i_q)i_d^*}{\Psi_d(i_d) - L_{qq}i_d^*}$, $x'_2 = \frac{-L_{dd}(i_d)i_q^*}{\Psi_d(i_d) - L_{qq}(i_q)i_d^*}$, $\dot{\mathbf{i}}_1^* = \begin{bmatrix} \dot{i}_d^* \\ \dot{i}_{q1}^* \end{bmatrix}$, $\dot{i}_{q1}^*$ can be obtained from (8) after substitution (15) and modifying fluxes.

Control algorithm without cross-coupling and saturation compensation. Control algorithm is based on the model with linearized magnetic system. The model can be derived from (1), (2) by means of substitution

$$\Psi_d(i_d) = \Psi_M + L_{dd}i_d, \Psi_q(i_q) = L_{qq}i_q, \tag{17}$$

where Ψ_M is flux from permanent magnets, inductances L_{dd}, L_{qq} are constants.

Algorithm for IPMSM speed control based on the model with linearized magnetic system was presented in [12]. Speed and current controllers are presented below. Controllers for the SynRM are the same if PM flux is considered to be zero.

Speed controller is

$$\begin{aligned} i_q^* &= \frac{1}{\mu\left(i_d^*\right)}\left(\frac{\nu}{J}\omega^* + \dot{\omega}^* + \hat{T}_L - k_\omega\tilde{\omega}\right), \\ \dot{\hat{T}}_L &= -k_{\omega i}\tilde{\omega}, \end{aligned} \tag{18}$$

where $\mu\left(i_d^*\right) = \frac{3}{2J}p_n\left(\left(L_{dd} - L_{qq}\right)i_d^* + \Psi_M\right) > 0$.

Derivative is required for the current controller is shown below

$$\begin{aligned} \dot{i}_{q1}^* = {} & \frac{1}{\mu\left(i_d^*\right)}\left(\frac{\nu}{J}\dot{\omega}^* + \ddot{\omega}^* + \dot{\hat{T}}_L\right) - \\ & -\frac{k_\omega}{\mu\left(i_d^*\right)}\left(-\left(\frac{\nu}{J} + k_\omega\right)\tilde{\omega} + \mu\left(i_d^*\right)\tilde{i}_q + \frac{3}{2J}p_n\left(\left(L_{dd} - L_{qq}\right)\tilde{i}_d i_q\right)\right) - \\ & -\frac{3}{2J}\frac{p_n\left(\left(L_{dd} - L_{qq}\right)\dot{i}_d^*\right)}{\mu^2\left(i_d^*\right)}\left(\frac{\nu}{J}\omega^* + \dot{\omega}^* + \hat{T}_L - k_\omega\tilde{\omega}\right), \end{aligned} \tag{19}$$

Current controllers are presented in matrix form

$$\begin{aligned} \mathbf{u} &= R\mathbf{i}^* - p_n\omega\mathbf{J}\boldsymbol{\Psi}'' + \mathbf{L}''\left(\dot{\mathbf{i}}_1^* - \mathbf{K}_i\tilde{\mathbf{i}} - \mathbf{x}\right) \\ \dot{\mathbf{x}} &= \mathbf{K}_{ii}\tilde{\mathbf{i}} \end{aligned} \tag{20}$$

where $\boldsymbol{\Psi}'' = \begin{bmatrix} \Psi_M + L_{dd}i_d \\ L_{qq}i_q \end{bmatrix}$, $\mathbf{L}'' = \begin{bmatrix} L_{dd} & 0 \\ 0 & L_{qq} \end{bmatrix}$.

In the next section presented algorithms will be compared and analyzed by means of simulation.

Simulation comparison. Simulation results are presented for IPMSM motor whose rated data is presented in the Appendix. Fluxes and inductances curves for the tested motor are presented in fig.1.

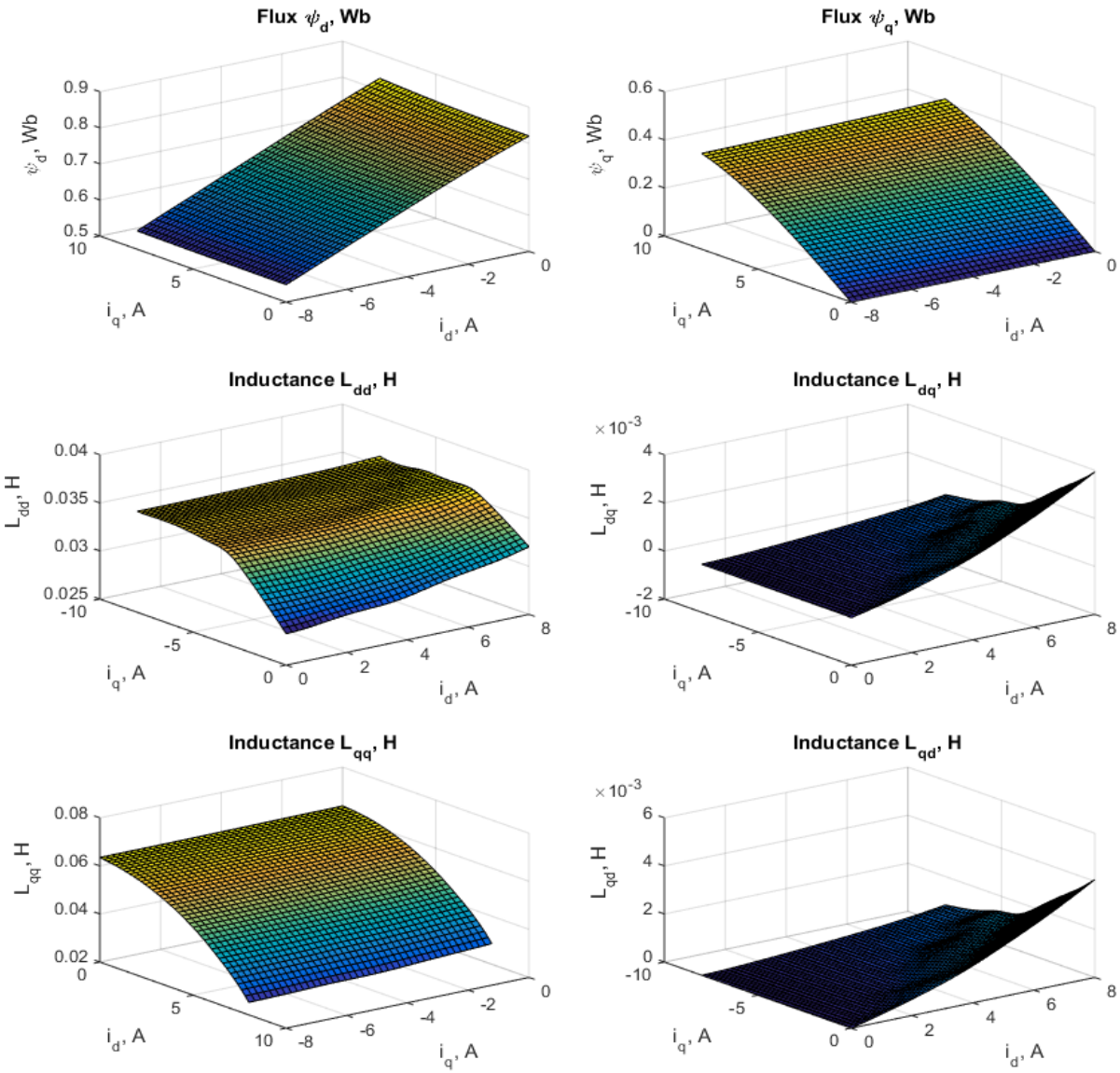

Figure 1 – Fluxes and inductances curves

Following test is proposed for algorithms comparison:

1. The motor speed reference trajectory ω^* starts from zero initial value at $t = 0.2s$ and reaches steady state value of 100rad/s at $t = 0.28s$ with the first and the second derivatives $1667 rad/s^2$ and $83000 rad/s^3$. At time $t = 0.8s$ speed trajectory reverses and reaches steady state value of –100rad/s at $t = 0.94s$. Deceleration to zero speed starts at time $t = 1.2s$ and lasts for 0.08s.

2. Direct current reference trajectory starts increasing at time $t = 0.35s$ and reaches steady state value of –2A at time 0.4s. Decreasing of the current reference trajectory starts at $t = 0.6s$ and ends with zero reference with transient duration of 0.05s.

3. Constant rated load torque $T_L = 20Nm$ is applied at 0.5s and at time $t = 1.1s$ load torque is set to zero.

Controller gains are tuned using standard consideration for the linear second orders systems and are the same for full compensation, only saturation compensation

and based on the model with linear magnetic system control algorithms: $k_i = 1000$, $k_{ii} = k_i^2 / 4$, $k_\omega = 200$, $k_{\omega i} = k_\omega^2 / 4$.

Test is simulated for three algorithms. Results for algorithm based on the model with linear magnetic system are presented in Fig. 2; for algorithm with only saturation compensation – in Fig. 3; for algorithm with full compensation of saturation and cross-coupling - in Fig. 4.

The control algorithm based on the model with linear magnetic system is characterized by zero speed error during reference tracking and about of 7rad/s when load torque is applied and removed. Quadrature current error is only 0.7A when load torque is applied and removed with small current fluctuations during transients, while i_d current error doesn`t exceed values of 0.01A, with low fluctuations.

In case of algorithm with only saturation compensation can be obtained slightly improved i_d and i_q currents dynamics. Speed tracking error and i_q current error during load torque compensation is the same.

In case of algorithm with full compensation speed tracking is slightly improved. Direct axis current error $\tilde{i}_d$ equals to zero during whole test. Transients during load torque compensation is the same as for other algorithms.

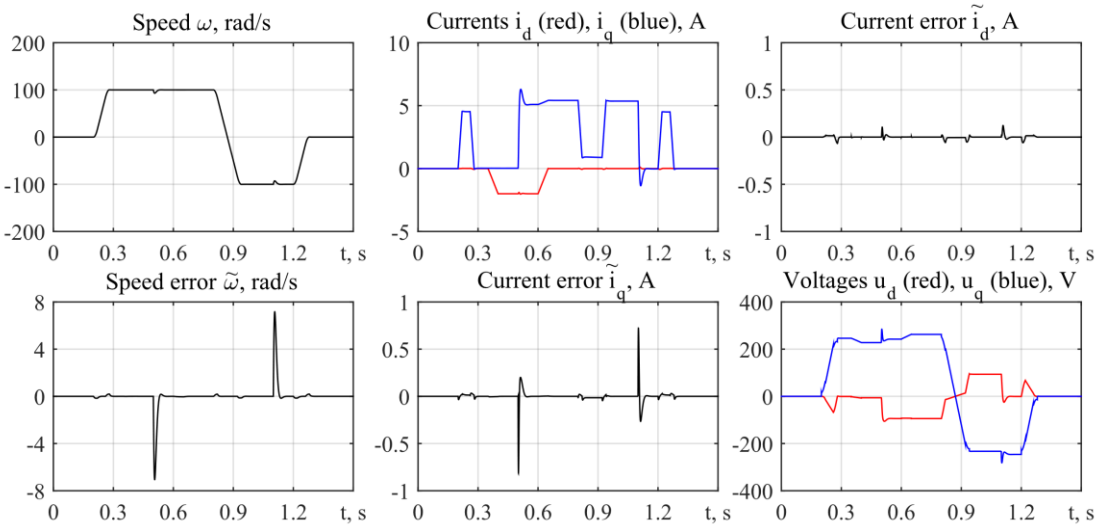

Figure 2 – Simulation transients for algorithm based on the model with linear magnetic system

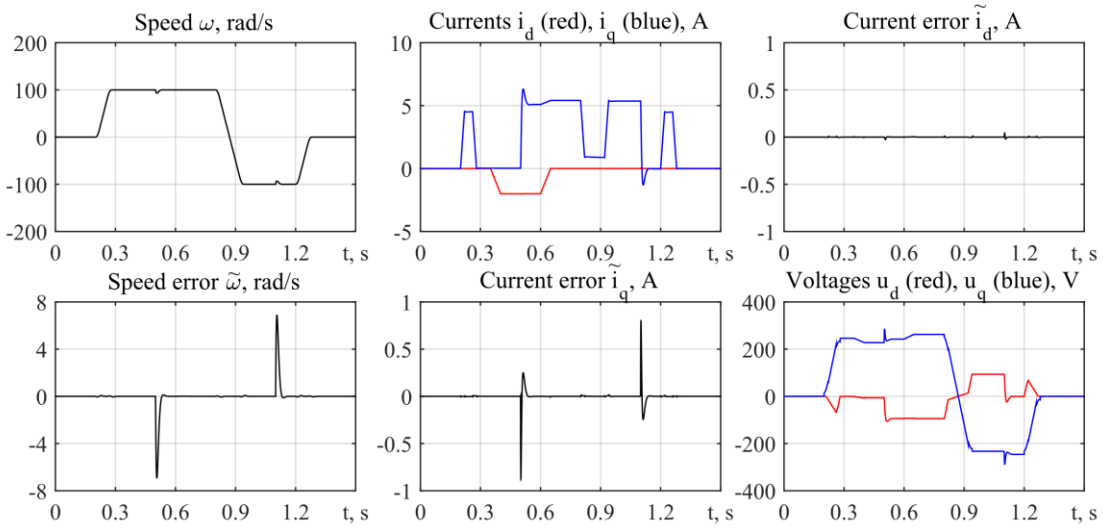

Figure 3 – Simulation transients for algorithm with only saturation compensation

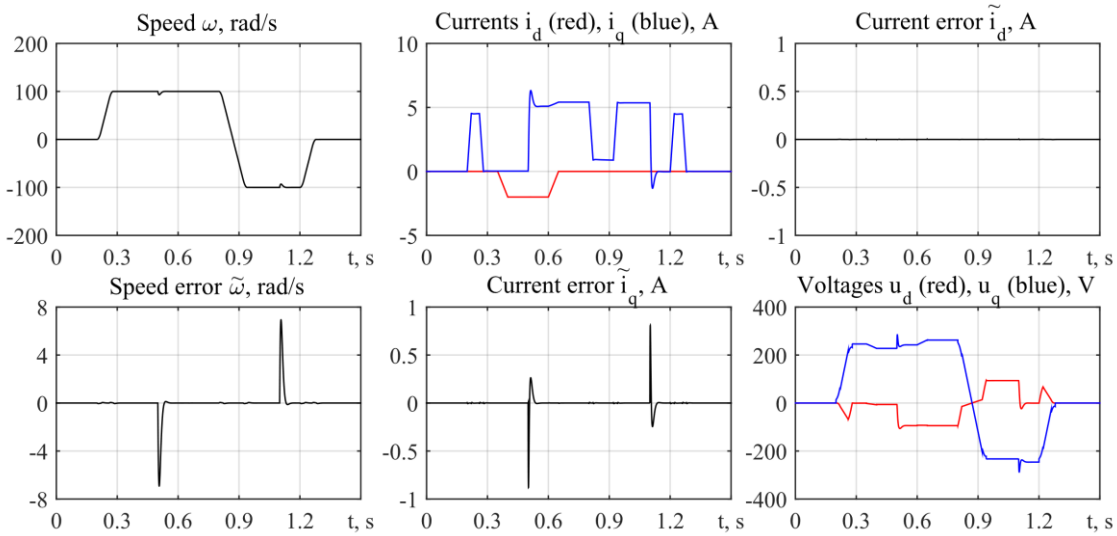

Figure 4 – Simulation transients for algorithm with saturation and cross-coupling compensation

Conclusions. In the paper, three speed tracking algorithms for salient pole synchronous motors are presented. Nonlinearities of motor magnetic system are considered in the algorithms to a different extent. Presented algorithms can be applied for both IPMSMs and SynRMs. Algorithm with saturation and cross-coupling compensation allows achieving full decoupling on speed and direct axis current control subsystems. On the other hand, comparison of the proposed algorithms shows that consideration of saturation and cross-coupling in the algorithm does not lead to significant improvements in performance. Moreover, realization of such algorithms requires not only full information about motor magnetic system, but also much higher computational efforts. Therefore, usage of algorithms where nonlinearities of the magnetic systems are considered is recommended only for extremely high-precision applications.

Appendix. Rated data of the tested IPMSM: $P_r = 2.2\text{kW}$, $\omega_r = 1000\,\text{r/min}$, $I_r = 5.6\text{A}$, $R = 2.75\text{Ohm}$, $L_{dd} = 35\text{mH}$, $L_{qq} = 54\text{mH}$, $\Psi_M = 0.86\text{Wb}$, $p_n = 3$.

References

1. S. Kim, Y. Yoon, S. Sul and K. Ide, "Maximum Torque per Ampere (MTPA) Control of an IPM Machine Based on Signal Injection Considering Inductance Saturation," in *IEEE Transactions on Power Electronics*, vol. 28, no. 1, pp. 488-497, Jan. 2013.

2. Jung Chul Kim, Jung Ho Lee, In Soung Jung and Dong Seok Hyun, "Vector control scheme of synchronous reluctance motor considering iron core loss," in *IEEE Transactions on Magnetics*, vol. 34, no. 5, pp. 3522-3527, Sept. 1998.

3. Bimal K. Bose, *Modern power electronics and ac drives*. The University of Tennessee, Knoxville: Condra Chair of Excellence in Power Electronics, 2001.

4. H. Nagura, Y. Iwaji, J. Nakatsugawa and N. Iwasaki, "New vector controller for PM motors which modeled the cross-coupling magnetic flux saturation," *The 2010 International Power Electronics Conference - ECCE ASIA -*, Sapporo, 2010, pp. 1064-1070.

5. S. Kim, Y. Yoon, S. Sul and K. Ide, "Maximum Torque per Ampere (MTPA) Control of an IPM Machine Based on Signal Injection Considering Inductance Saturation," in *IEEE Transactions on Power Electronics*, vol. 28, no. 1, pp. 488-497, Jan. 2013.

6. W. Xu and R. D. Lorenz, "High-Frequency Injection-Based Stator Flux Linkage and Torque Estimation for DB-DTFC Implementation on IPMSMs Considering Cross-Saturation Effects," in *IEEE Transactions on Industry Applications*, vol. 50, no. 6, pp. 3805-3815, Nov.-Dec. 2014.

7. K. Shin, J. Choi and H. Cho, "Characteristic Analysis of Interior Permanent-Magnet Synchronous Machine With Fractional-Slot Concentrated Winding Considering Nonlinear Magnetic Saturation," in *IEEE Transactions on Applied Superconductivity*, vol. 26, no. 4, pp. 1-4, June 2016, Art no. 5200404.

8. M. Fasil, C. Antaloae, N. Mijatovic, B. B. Jensen and J. Holboll, "Improved dq-Axes Model of PMSM Considering Airgap Flux Harmonics and Saturation," in *IEEE Transactions on Applied Superconductivity*, vol. 26, no. 4, pp. 1-5, June 2016, Art no. 5202705.

9. K. Lee and J. Ha, "Dynamic decoupling control method for PMSM drive with cross-coupling inductances," 2017 *IEEE Applied Power Electronics Conference and Exposition (APEC)*, Tampa, FL, 2017, pp. 563-569.

10. M. H. Mohammadi and D. A. Lowther, "A Computational Study of Efficiency Map Calculation for Synchronous AC Motor Drives Including Cross-Coupling and Saturation Effects," in *IEEE Transactions on Magnetics*, vol. 53, no. 6, pp. 1-4, June 2017, Art no. 8103704.

11. Rodkin D., Zinchenko O., Peresada S. "Survey of the interior permanent magnet synchronous motor models considering saturation and cross-magnetization", International scientific and technical journal of young scientists, graduate students and students "MODERN PROBLEMS OF ELECTRIC POWER ENGINEERING AND AUTOMATION", Kyiv, Ukraine, 2020

12. S. Peresada, V. Reshetnyk, D. Rodkin, O. Zinchenko, "Linearizing speed control and self-commissioning of interior permanent magnet synchronous motors", Bulletin of the National Technical University "KhPI". Problems of automated electrodrive. Theory and practice, Kharkiv, 2019. no. 9, vol. 1334. pp. 36-42. (in Ukrainian).